Click Chemistry Functionalized Polymeric Nanoparticles Target Corneal Epithelial Cells through RGD-Cell Surface Receptors

Jiao Lu,[†] Meng Shi,[‡,§] and Molly S. Shoichet*[,†,‡,§]

Department of Chemistry, Department of Chemical Engineering and Applied Chemistry, and Institute for Biomaterials and Biomedical Engineering, Terrence Donnelly Center for Cellular and Biomolecular Research, University of Toronto, 160 College Street, Room 514, Toronto, Ontario M5S 3E1. Received July 24, 2008; Revised Manuscript Received November 17, 2008

Self-assembled polymeric nanoparticles modified with targeting ligands on the surface provide a means for localized cell delivery. To gain greater insight into the possibility of derivatizing poly(2-methyl-2-carboxytrimethylene carbonate-*co*-D,L-lactide) (poly(TMCC-*co*-LA)) nanoparticles using the Huisgen's 1,3 dipolar cycloaddition reaction, we synthesized amphiphilic copolymers comprising a hydrophobic poly(TMCC-*co*-LA) backbone and a hydrophilic poly(ethylene glycol) (PEG) pendant chain. By coupling amine-terminated PEG-azide to the carboxylic acid group of the poly(TMCC-*co*-LA) via EDC chemistry, an amphiphilic copolymer was formed. The poly(TMCC-*co*-LA)-*g*-PEG-N_3 self-assembled in aqueous solution and presented azide groups on the surface of the nanoparticles. Alkyne-modified KGRGDS peptides were synthesized and coupled to the azide-functionalized nanoparticles via Huisgen's 1,3 dipolar cycloaddition, which was catalyzed by copper sulfate and sodium ascorbate in aqueous solution. Using coumarin-modified lysine (K) of the KGRGDS peptide, fluorescence was used to determine that there were approximately 400 peptides bound to each nanoparticle. The bioactivity of the GRGDS nanoparticle was confirmed with a competitive cell attachment assay using rabbit corneal epithelial cells. This GRGDS-nanoparticle system may be suitable for targeted drug delivery.

INTRODUCTION

Peptides have attracted significant attention because of their diverse biological functionalities. For example, the Arg-Gly-Asp (RGD) containing motif is known to be vital for integrin-receptor mediated cell attachment, which influences cell migration, growth, and differentiation (*1*). The specific binding between RGD-containing peptides and their integrin receptors also plays an important role in cell targeting. The application of RGD-modified nanoparticles (NP) for endothelium targeting has been broadly studied (*2, 3*), specifically in the context of tumor vasculature, which undergoes continuous angiogenesis. RGD peptides can be used to prevent integrins from binding to their respective ligands, thereby causing apoptosis of endothelial cells of newly formed blood vessels (*4*).

Few studies have explored the use of RGD-containing nanoparticles for targeted delivery to the eye, yet fibronectin accumulates in the corneal epithelium after injury (*5*). In wound healing, the binding between RGD motifs on fibronectin and the $\alpha_v\beta_1$ integrin on the surface of corneal epithelial cells plays an important role in cell spreading and migration upon stimulation by epidermal growth factor (EGF) (*6*). Several features of the cornea profoundly reduce the efficiency of gene transfer or drug absorbance (*7, 8*) including the low permeability of the intact epithelial layer and the rapid secretion of tears. However, the delivery of ophthalmic drugs using polymeric nanoparticles engineered with targeting molecules, such as RGD-containing peptides, is promising for the treatment of a wide range of corneal epithelial defects such as corneal neovascularization, dystrophies, neurotrophic keratopathy, recurrent erosion, and dry eye syndrome, among others (*9*). Thus, coupling RGD-containing peptides to nanoparticles may provide a method for targeted drug delivery to the eye after injury.

Building on our previous experience with self-assembling polymers (*10*), we investigated the use of "click chemistry" to surface-functionalize novel nanoparticles with RGD peptides. The term "click chemistry" was first introduced by Sharpless et al. in 2001 to included those reactions that are broad in scope, have high yields, and are simple in product isolation, stereospecific, and compatible with both organic and aqueous reaction conditions (*11*). While "click chemistry" has come to include Diels−Alder among other coupling chemistries, Sharpless defined it as two small units being joined together with heteroatom links and fulfilling the above requirements. Among all the carbon−heteroatom bond formation reactions, the copper-catalyzed Huisgen 1,3-dipolar cycloaddition is the premier example of click chemistry and is known for its high degree of selectivity and stability (*11*). Moreover, the resulting triazole ring itself has been shown to possess a variety of biological functions including anti-HIV, antibacterial, and potent antihistamine activity (*12*−*14*). To take advantage of this click chemistry, we synthesized alkyne-KGRGDS and azide polymeric nanoparticles and reacted them together.

On the basis of the previous development of a novel copolymer backbone of poly(2-methyl-2-carboxytrimethylene carbonate-*co*-D,L-lactide) (poly(TMCC-*co*-LA)) (*15*), we coupled amine-terminated PEG-azide via EDC chemistry to the carboxylic acid groups of TMCC. The known properties of PEG, including water solubility, hydophilicity, and resistance to protein adsorption, make the polymer-*graft*-PEG structure highly desirable for biomaterial and drug delivery applications (*16*). This poly(TMCC-*co*-LA)-*g*-PEG-N_3 copolymer self-assembled to nanoparticles in aqueous solution and presented azide groups on the surface for further modification with alkyne-KGRGDS peptides by click chemistry (Scheme 1). The bioactivity of the peptide-modified nanoparticles was tested with rabbit corneal

* To whom correspondence should be addressed. 160 College, Room 514 Toronto, Ontario, M5S 3E1. Phone: 416-978-1460. Fax: 416-978-4317. E-mail: molly.shoichet@utoronto.ca.
[†] Department of Chemistry.
[‡] Department of Chemical Engineering and Applied Chemistry.
[§] Institute for Biomaterials and Biomedical Engineering.

10.1021/bc8003167 CCC: $40.75
Published on Web 12/18/2008

Scheme 1. Immobilization of Alkyne-KGRGDS Peptides on Nanoparticles by the Aqueous Huisgen'S 1,3 Dipolar Cycloaddition Reaction, Catalyzed by Copper Sulfate and Sodium Ascorbate (Room Temperature, 5 h)

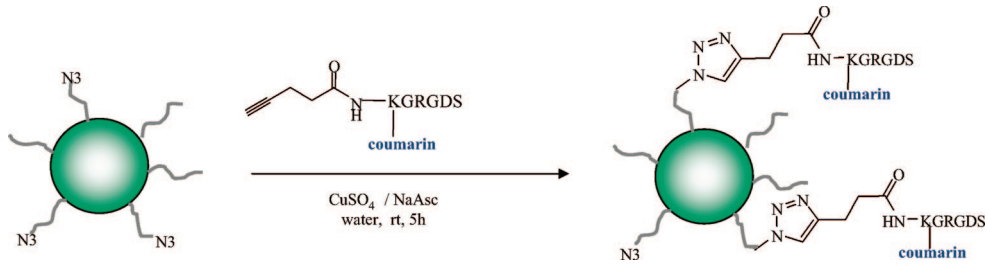

epithelial cells using a competitive cell attachment assay. To the best of our understanding, this is the first time that peptide-modified nanoparticles have been designed for targeted delivery to corneal epithelial cells.

EXPERIMENTAL PROCEDURES

Materials and Methods. The ^{1}H NMR spectra were recorded at 400 MHz at room temperature using a Varian Auto X8308−400 spectrometer. All the chemical shifts are in ppm. Molecular weights and polydispersity indices were measured by gel permeation chromatography (GPC) in THF relative to polystyrene standards on a system equipped with two-column sets (Viscotck GMHHR-M and Viscoteck GMHHR-H) and a triple detector array (TDA302) at room temperature with a flow rate of 0.6 mL/min THF eluent. Dynamic light scattering (DLS) measurements were performed using the Brookhaven 90Plus Particle Size Analyzer (Brookhaven Instruments, USA), which was operated at 647 nm at a scattering angle of 90°. Nanoparticle samples were suspended at 0.5 mg/mL in distilled water before the measurement. Cumulant analysis of light scattering data was used to estimate the hydrodynamic diameter and polydispersity of the nanoparticles. When the polydispersity equals zero, the sample is monodisperse, and as polydispersity increases so does the width of the distribution. As a general rule, nanoparticles are considered to have narrow size distributions when polydispersity is less than 0.025, and cumulant analysis works best when polydispersity is ≤0.3. (Additional information is available from Brookhaven.) The dry nanoparticle size was estimated by measuring the average diameter of 50 nanoparticles from images taken in the scanning transmission electron microscope (STEM) mode of the Hitachi S-5200 scanning electron microscope system operating at 30 kV. Samples were prepared by placing one drop of self-assembled nanoparticle solution (0.5 mg/mL in distilled water) on a carbon support film (Electron Microscopy Sciences, PA, USA). Excess solution was drained, and the sample was allowed to air-dry. The presence of an azide functional group was characterized by Nicolet Avatar 370 FTIR (Thermo Instruments Canada Inc.). The RGD-containing peptides were synthesized by solid-phase synthesis using a Pioneer Peptide Synthesis System (Foster City, CA, USA) using standard Fmoc/ HATU chemistry. The synthesized peptides were purified by HPLC (Jupiter 5 μ, C 18, 300 Å, 250 × 21.2 mm) using a gradient mixture of acetonitrile with 0.1% TFA and water. The gradient of acetonitrile with 0.1% TFA increased from 10% (10 min) to 30% (30 min) and finally to 90% (10 min). The Sephadex G-25 column was prepared according to the following procedures: Sephadex G-25 beads was soaked in 0.01 M PBS buffer at pH 7.4 overnight prior to packing the column (2.5 × 10 cm). The column was washed with the same PBS buffer for 1 h before use. The flow rate is determined by gravity. The Sepharose C4B column (5 × 15 cm) was prepared in the same manner as Sephades G-25 column, except distilled water was used instead of PBS buffer. Fluorescence intensity of coumarin was measured by a fluorescent microplate reader (SpectraMax GeminiEM, Molecular Device, USA) at excitation and emission wavelengths of 340 and 405 nm, respectively. The concentration of nanoparticles was measured by their absorbance in Bradford reagent (*10*) at 595 nm using a microplate reader (VersaMax, Molecular Devices, USA). Triplicate samples of equal volumes of NP solution and Bradford reagent were mixed in a clear 96-well plate at room temperature. After incubating for 30 s, a reading was taken.

All solvents and reagents were purchased from Sigma-Aldrich and were used as received, unless otherwise noted. Amino acids including Fmoc-Lys(MCA)-OH were purchased from Novabiochem (CA, USA). Activators and resins were obtained from Applied Biosystems (CA, USA). The peptides for cell attachment assays, GRGDS (97.8% pure, 490.48 g/mol), were acquired from Genscript Corp (New Jersey, USA). The SIRC-rabbit corneal epithelial cell line, CCL-60, was obtained from American type Culture Collection (ATCC, USA). Difunctional *tert*-butoxycarbonyl-protected amine-PEG-activated acid was purchased from Nektar Theraputics (Birmingham, AL, USA). All regenerated cellulose (RC) membranes were purchased from Spectrum Laboratories Rancho Dominguex (CA, USA). All the dialysis procedures used 4 L of distilled water as the exchange solvent. The water was replaced every 2 h for the first 8 h. 96-well reacti-bind amine-binding, maleic anhydride activated plates and the blocking buffer were purchased from Pierce. The Quant iT Picogreen dsDNA assay kit and the protocol are available from Invitrogen (Burlington, ON). The protocol document number is MP 07581, revised December 20th, 2005.

Synthesis of PEG-Azide (PEG-N_3). As shown in Scheme 2, difunctional *tert*-butoxycarbonyl-protected amine-PEG-activated acid (BocNH-PEG-NHS; **1**; 3446 Da, 1.00 g) and azido-octaethyleneglycol-amine (438.52 Da, 0.50 g) were dissolved in 10 mL of DMF and stirred for 24 h at room temperature. The reaction mixture was purified by dialysis against distilled water at room temperature for 24 h using a regenerated cellulose (RC) membrane with a molecular weight cutoff (MWCO) of 1 kDa. The dialyzed solution was freeze−dried to yield BocNH-PEG-N_3 **2** (0.92 g, 82% yield) as a white solid, which was then deprotected in 6 mL of 70% TFA aqueous solution. After 2 h, the reaction mixture was diluted with 18 mL of water and purified again by dialysis, as described above. After freeze−drying, a white solid product **3** (0.59 g, 64%) was recovered. The presence of the terminal azide group and the C−O bond were characterized by a stretching frequencies at 2103 cm^{-1} and 1012 cm^{-1}, respectively, in the FTIR spectrum. MALDI-TOF-MS: 3727.2 (calc. 3727.52). ^{1}H NMR (D_2O): δ 3.68 (s). For ^{1}H NMR and FTIR spectra, see Supporting Information Figure S1 for compound **2** and Figures S2 and S11 for compound **3**.

Synthesis of Poly(TMCC-*co*-LA)-*g*-PEG-N_3. The synthesis of PEG-grafted copolymer was carried out as illustrated in Scheme 3. The poly(TMCC-*co*-LA) **4** was synthesized by bulk copolymerization as previously reported (*10*). Copolymer **4** (100 mg) was dissolved in DMF (5 mL) and 10 mM MES buffer

Scheme 2. Synthesis of H_2N-PEG-N_3 by Reacting NHS-Activated PEG Chains with Amine-Terminated Octaethylene Glycol-Azide Followed by BOC Deprotection

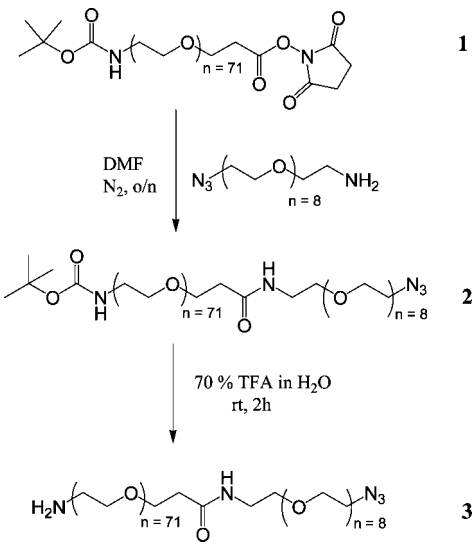

(0.5 mL, pH 5.5). *N*-ethyl-*N*′-(3-dimethylaminopropyl)carbodiimide hydrochloride (EDC, 10 wt %) and *N*-hydroxysulfosuccinimide (sulfo-NHS, 10 wt%) were then added, and the reaction solution was stirred at room temperature for 30 min. The PEG azide **3** (50 mg), dissolved in 0.5 M borate buffer (1 mL, pH 9.0), was slowly added to the activated copolymer solution under stirring. The reaction mixture was incubated at room temperature for 24 h, after which it was dialyzed against distilled water using an RC membrane at a MWCO of 12−14 kDa. The excess PEG was removed using a Sepharose C4B column equilibrated with distilled water. The collected fractions containing polymers were freeze−dried to give a white solid (55 mg, 50% yield). ^{1}H NMR (DMSO): δ 0.99 (br s, CH_3 from TMCC), 1.42−1.46 (m, CH_3 from LA), 3.49 (s, PEG), 4.19 (br s, methylene from TMCC), and 5.17−5.19 (m, CH from LA). ^{1}H NMR spectra of poly(TMCC-*co*-LA) **4** and poly(TMCC-*co*-LA)-*g*-PEG-azide **5** are shown in Supporting Information Figures S3 and S4.

Self-Assembly of Polymers to Nanoparticles by Dialysis. The nanoparticles **6** were prepared by self-assembly of poly(TMCC-*co*-LA)-*g*-PEG-azide by memberane dialysis, as previously reported (*15*). Briefly, copolymer **5** (15 mg) was dissolved in 1.5 mL of DMF/borate buffer (0.5 M, pH 9.0) at a volume ratio of 1.425 to 0.075. The solution was dialyzed against distilled water using a dialysis membrane with a MWCO of 12−14 kDa at room temperature for 8 h.

Synthesis of Alkyne-Modified KGRGDS. The synthesis of alkyne-modified KGRGDS peptide is shown in Scheme 4. The alkyne-modified KGRGDS was synthesized by solid-phase synthesis 4-pentynoic acid (0.20 g, 2 mmol) was activated by *N,N*′-diisopropyl carbodiimide (DIC, 1.24 mL, 8 mmol) in 10 mL of CH_2Cl_2 under N_2 for 30 min. Alkyne-KGRGDS was added, and the mixture was stirred at room temperature for another 2 h. The resin was filtered and washed with 20 mL each of dichloromethane, methanol, and isopropyl alcohol (IPA).

The resin recovered from the previous step was dissolved in TFA/water (9.5 mL/0.5 mL, v/v) and stirred for 2 h. The peptide dissolved in solution was separated from the resin by vacuum filtration and concentrated by rotary evaporation. The crude oily product was precipitated in 100 mL of cold ether and stored in a −80 °C freezer overnight. The precipitated white peptide (65 mg, 65% yield) was recovered by centrifugation and dried under N_2.

The product was further purified by HPLC to yield 50 mg of the final product as a white solid (yield 76%). The final product was confirmed by ^{1}H NMR and mass spectrometry (MS). ^{1}H NMR (D_2O, 400 MHz): δ 1.28−1.83 (m, 10H), 2.31 (s, 1H), 2.44 (m, 4H), 2.77−2.95 (m, 2H), 3.10−3.16 (t, 2H, J = 6 Hz), 3.18−3.22 (t, 2H, J = 6 Hz), 3.82−3.97 (m, 11H), 4.10−4.16 (dd, 1H, J_1 = 5 Hz, J_2 = 8 Hz), 4.26−4.32 (dd, 1H, J_1 = 5 Hz, J_2 = 8 Hz), 4.48−4.51 (dd, 1H, J_1 = 4 Hz, J_2 = 5 Hz), 4.79−4.81 (m, 1H) 6.30 (s, 1H), 6.99−7.02 (m, 2H), 7.62−7.64 (m, 1H). ESI-MS (MNa^+): 936.4 (calc. 937.38). (The same syntheses and characterization methods were used for the following additional peptides studied and are described in the Supporting InformationFigures S1−S8: alkyne-KGRGDS, scrambled alkyne-KGRDGS, alkyne-GRGDS, and scrambled alkyne-GRDGS.)

Immobilization of KGRGDS on Nanoparticles by Click Chemistry. Alkyne-modified KGRGDS, at concentrations of 25, 50, and 100 μg/mL, was reacted with poly(TMCC-*co*-LA)-*g*-PEG-azide nanoparticles (1.875 mg/mL) at room temperature in distilled water under catalysis with copper sulfate (0.6 μmol/mL) and sodium ascorbate (3.0 μmol/mL). The reaction mixture was stirred at room temperature for 1, 3, and 5 h (see Results and Discussion). It was then purified through a Sephadex G-25 column equilibrated with 0.01 M PBS buffer at pH 7.4.

Cell Attachment Assay. *GRGDS-Modified Cell Culture Plates.* The peptide sequence GRGDS in borate buffer (pH 9.0, 0.5 M) was placed in a 96-well reacti-bind amine-binding, maleic anhydride activated plates (100 μL/well) at a concentration of 100 μg/mL. The plate was incubated on a shaker at room temperature overnight, and the peptide solution was then removed. Protein blocking buffer (200 μL/well) was added and incubated for 1 h at room temperature to quench any remaining reactive maleic anhydride groups and block remaining open sites on the plate surface.

Preparation of Cells. SIRC-rabbit corneal epithelial cells were cultured in tissue culture plates with minimum essential medium α (α-MEM) containing 10% FBS, 1% penicillin/streptomycin, and 1% glutamine in an incubator (37 °C, 5% CO_2, 100% humidity). Before harvesting, cells were incubated with fresh cell culture medium containing with 10 ng/mL of epidermal growth factor (EGF) overnight.

Competitive Cell Attachment Assay. To test the binding affinity of the GRGDS-modified nanoparticles, the attachment of cells to GRGDS-modified cell culture wells was tested after preincubation with either GRGDS-nanoparticles or scrambled GRDGS-nanoparticles and compared to the cell attachment observed when cells were preincubated in soluble GRGDS. Specifically, a cell suspension of cultured rabbit corneal epithelial cells with an equal volume of 1 or 10 μg/mL of GRGDS or 2.0 mg/mL of peptide-modified nanoparticles with peptide concentration of 5.5 μg/mL in PBS buffer (0.01 M, pH 7.4) was preincubated at 37 °C for 30 min before plating into wells (1×10^4 cells/well, 100 μL). The cells were incubated at 37 °C for another 4 h after plating. The wells were then washed three times with fresh cell culture medium before quantifying the number of attached cells using the PicoGreen assay. It was assumed that every cell contained 7.7 pg of DNA.

RESULTS AND DISCUSSION

Synthesis of Poly(TMCC-*co*-LA)-*g*-PEG. The amphiphilic copolymer, poly(TMCC-*co*-LA)-*g*-PEG-azide, was designed specifically for the creation of RGD-nanoparticles by combining strategies of polymeric self-assembly and click chemistry of bioconjugation in one process. The copolymer is biodegradable and biocompatible for in vivo applications, amphiphilic with the ability to self-assemble into ordered structures, and capable

Scheme 3. Synthesis of Poly(TMCC-*co*-LA)-*g*-PEG-Azide[a]

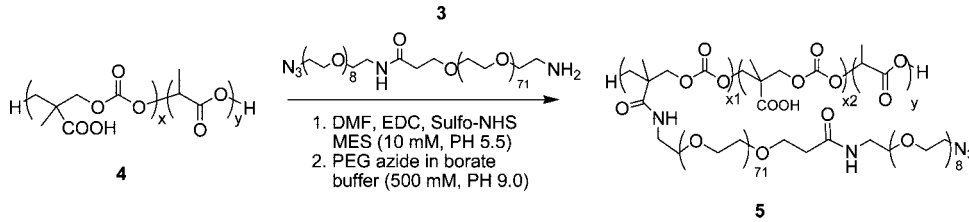

[a] The carboxylic acid groups on the copolymer backbone were first activated with *N*-(3-dimethylaminopropyl)-*N*′-ethylcarbodiimide hydrochloride (EDC) and *N*-hydroxysulfosuccinimide (Sulfo-NHS) for 30 min. Then, amine-terminated PEG azide was covalently bound under basic conditions overnight.

Scheme 4. Synthesis of the Alkyne-Modified KGRGDS Peptides[a]

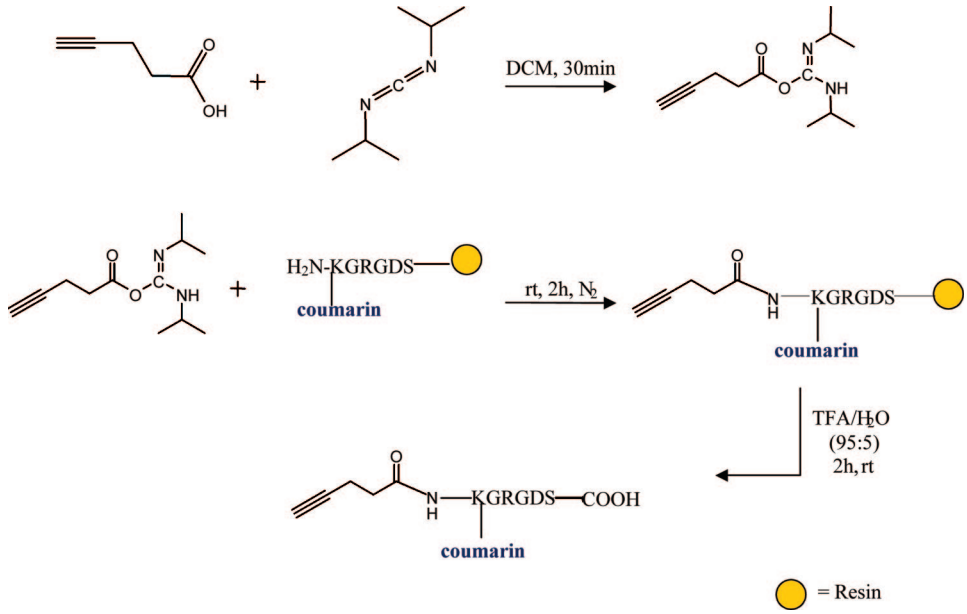

[a] 4-Pentynoic acid was activated by *N,N*′-diisopropylcarbodiimide (DIC) for 30 min and reacted with amine-terminated peptides. The peptide was cleaved from the resin using a 95% TFA aqueous solution for 2 h at room temperature.

of click chemistry chemistry due to the presence of azide groups at the PEG terminus.

The number average molecular weight and polydispersity of poly(TMCC-*co*-LA) were determined by GPC (see Supporting Information Figure S10), relative to polystyrene standards in THF, to be 30.4 kDa and 2.7, respectively. The molar percentage of TMCC in the copolymer was determined from ^{1}H NMR data to be 9.3% by comparing the integrated peak of TMCC methylene (4.18 ppm) with that of the LA methine (5.13−5.19 ppm). This number is slightly lower than the feed ratio (TMCC/D,L-lactide 10/45), where each D,L-lactide monomer contains two repeat units. This is probably because LA is more reactive than TMCC in the copolymerization, leading to an enrichment of LA in the copolymer (*17*). The random copolymer composition was estimated from ^{1}H NMR and GPC data to be poly(TMCC)$_{32}$-*co*-(LA)$_{310}$.

After copolymerization, the carboxylic acid groups along the copolymer chain were deprotected, allowing for further functionalization with PEG-N_3 using EDC chemistry. This resulted in amphiphilic copolymers of poly(TMCC-*co*-LA)-*g*-PEG-azide with well-defined hydrophobic and hydrophilic segments. The ratio of PEG grafted to poly(TMCC)$_{32}$-*co*-(LA)$_{310}$ was estimated by comparing the integrated peak areas from the ^{1}H NMR spectrum of PEG methylene (3.49 ppm) to that of the TMCC methylene (4.18 ppm). On average, there was approximately one PEG chain grafted to every poly(TMCC)$_{32}$-*co*-(LA)$_{310}$ backbone. The number average molar mass of poly(TMCC)$_{32}$-*co*-(LA)$_{310}$-*g*-PEG was calculated according to

$$M_{\text{n (poly(TMCC}-co-\text{LA)}-g-\text{PEG)}} = M_{\text{n (backbone)}} + (M_{\text{n (PEG)}} \times \#\text{ of PEG per copolymer backbone}) \quad (1)$$

Given that $M_{\text{n(backbone)}}$ is 30.4 kDa, $M_{\text{n(PEG)}}$ is 3.40 kDa and there is one PEG chain per copolymer backbone; the $M_{\text{n (poly(TMCC-}co\text{-LA)-}g\text{-PEG)}}$ is estimated at 33.8 kDa.

Estimation of the Molecular Weight of Nanoparticles (M_{NP}) and the Number of Chains Aggregated in a Nanoparticle (N_{agg}). When poly(TMCC-*co*-LA)-*g*-PEG was dissolved in DMF with 5% borate buffer and dialyzed against water (see Experimental Procedures), the hydrophobic poly(TMCC-*co*-LA) backbone self-assembled to form the nanoparticle core, while the hydrophilic PEG chains interacted with the surrounding water to form the nanoparticle shell. As observed by dynamic light scattering (DLS), the resulting self-assembled nanoparticles had an average diameter of 130.8 nm and a polydispersity index (PDI) of 0.2897, which indicates that the nanoparticles are polydisperse. By scanning transmission electron microscopy, the average diameter of the nanoparticles was 87.4 ± 12.5 nm (n = 50 nanoparticles, mean ± s.d.). The STEM image has been previously reported (*10*). The diameter measured by STEM is smaller than that measured by DLS, because STEM imaged the dry nanoparticles, whereas DLS detected the hydrated nanoparticles in aqueous solution. While the DLS data

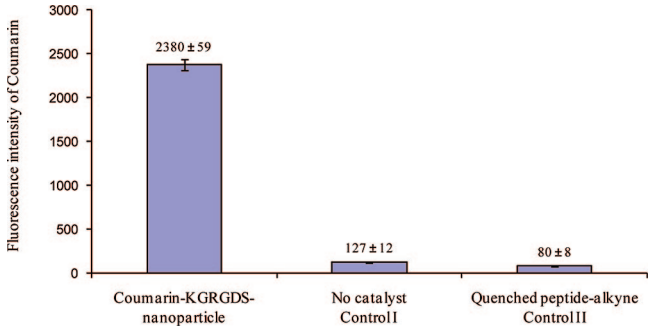

Figure 1. The fluorescence intensity of coumarin was readily detected on azide-functionalized nanoparticles that had reacted with alkyne-peptide in the presence of copper sulfate and sodium ascorbate. In control I, the identical incubation between peptides and nanoparticles was repeated in the absence of copper sulfate and sodium ascorbate, demonstrating the importance of the catalyst for successful peptide modification. In control II, peptides were preincubated with 4-azidoaniline for 3 h before incubating with nanoparticles and catalyst, demonstrating that alkyne groups were quenched and unavailable for reaction with nanoparticle-azide.

are a better measure of the hydrated nanoparticle diameter, the standard deviation of the mean calculated from the STEM data is likely a better indication of the polydispersity of the nanoparticles (*10*). Assuming that the dried nanoparticle is a hard sphere with negligible porosity, the molar mass of the nanoparticle M_{NP} can be calculated from

$$M_{NP} = \frac{4\pi R^2 N_A}{3\upsilon_2} \quad (2)$$

where R is the radius of the nanoparticle (43.7 ± 6.3 nm from STEM); υ_2 is the partial specific volume of the polymer, which is estimated at 0.95 mL/g, and N_A is Avogadro's constant (6.02×10^{23}) (*18*). The average nanoparticle aggregation number, N_{aggs}, can be estimated as

$$N_{agg} = M_{NP}/M_{n(\text{poly(TMCC-}co\text{-LA)-}g\text{-PEG})} \quad (3)$$

using the value of M_{NP} calculated from eq 2.

Thus, one nanoparticle comprises approximately (6.5 ± 0.4) $\times 10^3$ polymer chains.

Immobilization of Alkyne-KGRGDS on Azido-Nanoparticles by Click Chemistry. In the self-assembled nanoparticle system, the azide-alkyne Huisgen's cycloaddition reaction was designed to occur at the interface between the azide-PEG corona of the nanoparticles and the aqueous phase in which alkyne-peptides were dissolved. After the amphiphilic copolymer self-assembled into nanoparticles, the hydrophilic segments oriented outward to the water phase. The terminal azide groups are accessible to alkyne-functionalized molecules in the aqueous solution, enabling click chemistry at the PEG terminus of the self-assembled nanoparticles. Coumarin-modified alkyne-KGRGDS was reacted with azide-nanoparticles at room temperature for 5 h in the presence of copper sulfate and sodium ascorbate. To confirm the Huisgen's 1,3 dipolar cycloaddition reaction, two controls were carried out: (1) the reaction was carried out in the absence of catalyst; and (2) the reaction was carried out after quenching the alkyne groups on KGRGDS with a large excess of 4-azidoaniline.

The fluorescence of the coumarin-modified alkyne-KGRGDS was used to measure the success of the reaction between peptide-alkyne and azido-nanoparticle. As shown in Figure 1, nanoparticles incubated with an excess of alkyne-KGRGDS showed a strong fluorescent signal at (2380 ± 59) indicating that the fluorescent peptide was coupled to the nanoparticles. Neither the control group lacking the copper sulfate/ascorbic acid (127 ± 12) nor that with quenched peptide-alkyne (80 ± 8) showed significant fluorescence. Together, these data confirmed the successful Huisgen's 1,3 dipolar cycloaddition reaction between peptide-alkyne and azido-nanoparticle. The hydrodynamic diameter of the nanoparticles (130.8 nm), determined by DLS, did not change significantly after peptide modification (126.2 nm) where the PDI was 0.2879. This suggests that the nanoparticles do not aggregate as a result of peptide modification.

Estimation of the Amount of Peptides Per Nanoparticle. To estimate the amount of peptide coupled per nanoparticle, the concentrations of both peptide and nanoparticle were independently determined, relative to standard curves with known concentrations of peptides and nanoparticles. The concentration of peptide was measured by the fluorescence intensity associated with coumarin. The concentration of nanoparticles was measured by their absorbance in Bradford reagent (*10*) at 595 nm using a microplate reader. The number of peptides per nanoparticle (n) was estimated according to eq 4

$$n = \frac{\text{peptide[M]}}{\text{nanoparticle[M]}} \quad (4)$$

To determine the optimum reaction time and the maximum number of peptides that can be conjugated per nanoparticle, both the click chemistry reaction time and the alkyne-KGRGDS concentration were varied. In Figure 2a, azido-nanoparticles reacted with 7-fold molar excess of alkyne-KGRGDS catalyzed by copper sulfate and sodium ascorbate at room temperature for 1, 3, and 5 h. The amount of peptide per nanoparticle increased between 1 and 3 h, after which a plateau of 439 ± 11 (mean ± standard deviation) peptides per nanoparticle was achieved, demonstrating that the reaction was complete after 3 h. In Figure 2b, azido-nanoparticles reacted for 5 h with various concentrations of alkyne-KGRGDS, where the peptide to copolymer molar ratio increased from 2:1 to 7:1. As the peptide to polymer ratio increased, the amount of peptide bound per nanoparticle increased from 229 ± 2 to 406 ± 21. According to our calculation, each NP has approximately 6500 PEG groups, but only ~440 peptides immobilized. This low reaction yield may be explained by not all PEG chains having azido groups and some of the azido groups not being available for reaction due to steric interactions. For example, some of the azido groups may have been buried within the PEG corona. Although the yield for azide-alkyne Huisgen's cycloaddition reaction of small molecules is normally above 80% (*19*−*21*), the kinetics of this reaction are very different between small molecules and polymers. As reported, the yield of this reaction dropped below 50% when the cycloaddition reaction was performed between two polymers (*22*). The yield is expected to drop further with polymeric nanoparticles, where accessibility of the azido groups is limited by entangled polymer chains and steric hindrance associated with solid particles. The number of immobilized peptides per nanoparticle is comparable to literature values (*23*). While many of the PEG-azido groups are left unreacted, they are largely inert in cell culture, as has been previously shown with azido-sugars on the cell surface that were used for bioorthogonal chemistry (*28*). However, the click chemistry in this nanoparticle system is advantageous over other coupling methods described in the literature because of the specificity, speed, and relative ease of the reaction. While the Huisgen 1,3 dipolar cycloaddition reaction requires the introduction of alkyne and azide groups, the common thiol-maleimide Michael-type addition chemistry also requires the introduction of free thiol and maleimide groups. However, the ligation reaction of the thiol-maleimide occurs in the narrow pH range 6.5−7.5. If the pH is too high, hydrolysis of the maleimide will occur; if the pH is too low, the reaction will occur very slowly or not at all. Thiol groups are very reactive toward various electrophiles and rapidly deteriorate when in solution. A protecting group is usually introduced, followed by a deprotection step (*24*−*26*).

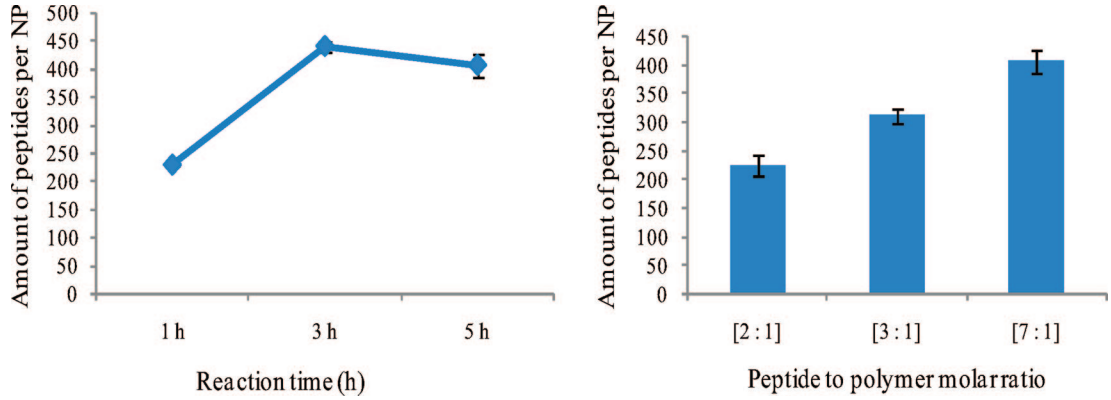

Figure 2. (a) Nanoparticles reacted with 7-fold molar excess of alkyne-KGRGDS catalyzed by copper sulfate and sodium ascorbate at room temperature for 1 h (229 ± 2), 3 h (439 ± 11), and 5 h (406 ± 21). (b) Nanoparticles reacted for 5 h with various concentrations of alkyne-KGRGDS where the peptide to copolymer molar ratio increased from 2:1 (224 ± 18) to 3:1 (311 ± 13) to 7:1 (406 ± 21). The numbers in parentheses are the means ± standard deviations for the number of peptides per nanoparticle.

Unlike the 3 h required for the click chemistry described herein, alternative coupling mechanisms, such as amine−aldehyde conjugation in the presence of the reducing agent, $NaBH_3CN$, has the disadvantage of requiring four days of reaction time (*27*) and the use of the highly toxic $NaBH_3CN$ reducing agent. Short reaction time, broad pH range, mild reaction conditions, and a simple purification process demonstrate the broad utility of click chemistry. Importantly, the click chemistry also allows us to couple the bioactive molecules (in this case, GRGDS peptides) in water after nanoparticle formation, thereby avoiding exposure of peptides (or proteins) to potentially denaturing organic solvents.

A clinically useful nanoparticle carrier for drug delivery, in addition to allowing surface modification, also has to be nontoxic, amenable to sterile filtration, and stable over a long period of time (*15*). Our nanoparticle system fulfills these criteria.

Cell Attachment Assay. Maleic anhydride functionalized 96-well plates were coated with amine-terminated GRGDS-containing peptides, and then, any unreacted sites were blocked with blocking buffer to ensure that GRGDS peptides were the only binding sites for corneal epithelial cells. To test the bioactivity of immobilized NP-GRGDS and the binding affinity between NP-GRGDS and corneal epithelial cells, a competitive cell attachment assay was performed, as shown quantitatively in Figure 3 and qualitatively in Supporting Information Figure S9. The number of corneal epithelial cells that adhered to the GRGDS-modified culture wells was quantified, comprising the positive control, as shown in Figure 3. The negative control, where the 96-well plate lacked the GRGDS peptide, showed very little cell adhesion. To better understand the binding affinity of this interaction, the epithelial cells were preincubated with soluble GRGDS peptides prior to plating on GRGDS-modified surfaces. As shown, cell attachment reduced from 70% to 40% compared to the positive control as the concentration of soluble GRGDS increased from 1 μg/mL to 10 μg/mL, indicating that the RGD integrin receptors on the cells were at least partially responsible for cell attachment. To determine the binding affinity of GRGDS bound to the nanoparticles, we repeated the preincubation study, replacing soluble GRGDS with NP-GRGDS.

When preincubated with NP-GRGDS prior to plating, fewer cells attached to the GRGDS-modified plate, similar to that observed when cells were preincubated with soluble GRGDS. The cell attachment was both significantly less than the positive control and similar to the negative control (where the cell plates lacked GRGDS). Importantly, the cell surface integrin−RGD interaction was confirmed with two controls: scrambled NP-GRDGS and NPs with blocked azido groups (i.e., no peptides). When the epithelial cells were preincubated with either scrambled NP-GRDGS or blocked NP-azido groups, the NPs did not sufficiently block the epithelial cell-surface integrin receptors, and thus, there were significantly more cells attached to the GRGDS-modified cell culture surfaces than had been observed when cells were preincubated with NP-GRGDS samples. However, there were fewer adherent cells after preincubation with either scrambled NP-GRDGS (1446 ± 377) or NP-blocked azido groups (1305 ± 215) relative to the positive control (1958 ± 214), which suggests some nonspecific binding of nanoparticles to cells.

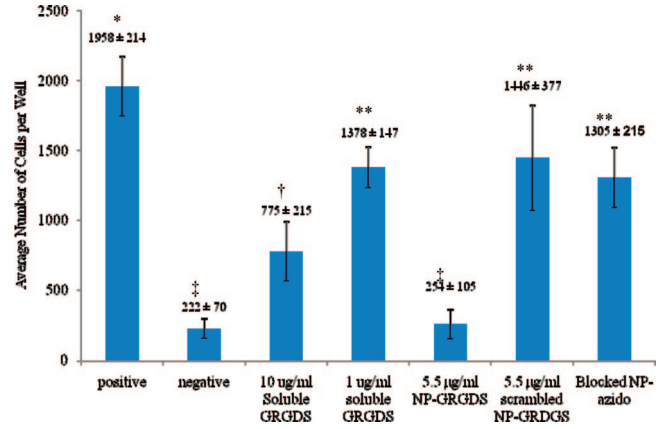

Figure 3. Competitive assay of rabbit corneal epithelial cell surface receptors to RGD. The positive control demonstrates a large number of cells bind to GRGDS-coated well-plate surfaces after a 4 h incubation. The negative control shows that few epithelial cells bind to unmodified well surfaces, demonstrating an RGD-mediated cell attachment. Competitive inhibition of cell attachment was demonstrated with soluble GRGDS (at concentrations of 10 and 1 μg/mL) where the number of adherent cells to the well plates decreased with increased GRGDS concentration. The bioactivity of the click chemistry bound NP-GRGDS (5.4 μg/mL) was confirmed by the similar competitive inhibition of cell attachment. The binding affinity of this interaction was verified with the scrambled NP-GRDGS (5.4 μg/mL) and nanoparticles with blocked azido groups where cell attachment was not inhibited. Shown are the mean ± standard deviation for $n = 3$ independent tests of triplicate assays; ANOVA was used for statistical analysis. The Posthoc analysis showed that there is a statistical difference ($p < 0.05$) between the different symbols.

Interestingly, NP-GRGDS samples seemed to be more effective at inhibiting epithelial attachment to the GRGDS-modified plates than soluble GRGDS, as demonstrated in Figure 3. While there is some nonspecific cell adhesion to the nanoparticles, as was observed with the NP controls, the NP-

GRGDS sample significantly reduced cell adhesion relative to the NP controls and the soluble GRGDS, indicating that additional mechanisms are required to explain the results. It is unlikely that there was any cytotoxicity associated with the remaining copper sulfate due to the small amount used, with our thorough purification methodology and literature demonstrating cell viability at 100−1000× greater copper concentrations (*29*). Thus, there are at least two possible explanations. The presence of multiple peptides on a given nanoparticle suggests multivalent interactions with the cells or avidity, as has been suggested by others (*23*). Alternatively, some of the soluble GRGDS peptides may have been internalized by the cells via an integrin-independent pathway, or even if by an integrin-dependent pathway, the integrin may have been recycled on the cell surface and available to interact with substrate-bound GRGDS-cell culture plates. A similar mechanism was observed by Castel et al. who showed that, at a concentration of 10 μg/mL, the RGD peptide targeted for $\alpha_v\beta_3$ was internalized in both α_v-integrin expressing and nonexpressing melanoma cells by an integrin-independent fluid-phase endocytosis pathway that did not alter the number of functional integrin receptors at the cell surface (*30*). This internalization occurred within 30 min at 37 °C. In our studies, relative to the soluble GRGDS, the NP-GRGDS effectively limited cell adhesion to the GRGDS coated well plates likely because it could not be internalized in the time frame studied due to the large particle size. Using confocal microscopy and fluorescent GRGDS-nanoparticles, we had no evidence for internalization (data not shown).

In order to improve the specificity and binding affinity of these GRGDS- nanopaticles, the synergistic proline-histidine-serine-arginine-asparagine (PHSRN) sequence can be similarly coupled to our nanoparticles, with the appropriate spacer between the two peptides (*31*)for optimal specificity with $\alpha_v\beta_1$ intergrins (*32*). Importantly, the platform conjugation technology described is applicable to a variety of peptides.

CONCLUSIONS

GRGDS peptides were successfully immobilized on self-assembled, polymeric nanoparticles using the azide-alkyne Huisgen 1,3 cycloaddition reaction. This chemistry is efficient and broadly applicable to a diversity of molecules. The azide-alkyne reaction was complete within 3 h and resulted in approximately 400 conjugated peptides per nanoparticle, allowing for interactions with cells that have $\alpha_v\beta_1$-integrin receptors up-regulated. The size of the nanoparticles detected by DLS was unchanged after peptide modification. The covalently bound NP-GRGDS peptides maintained their bioactivity and binding affinity with rabbit corneal epithelial cells relative to scrambled NP-GRDGS controls. These NP-GRGDS samples are small enough for sterile filtration and may be useful for targeted delivery to the injured eye.

ACKNOWLEDGMENT

We thank Professor Mitchell Winnik and Daniel Majonis for the use of their GPC, Dr. Neil Coombs for STEM imaging, and Ryan Wylie for helpful discussions. We are grateful to NSERC and CIHR for funding through the Collaborative Health Research Program.

Supporting Information Available: ^{1}H NMR data for compounds **2**−**5** and all the peptides, the cell images taken by inverted microscope, the GPC data for poly(TMCC-*co*-LA), and the IR spectrum for compound **3**. This material is available free of charge via the Internet at http://pubs.acs.org.

LITERATURE CITED

(1) Ruoslahti, E. (1996) RGD and other recognition sequences for integrins. *Annu. Rev. Cell Dev. Biol. 12*, 697–715.

(2) Kim, J. H., Kim, Y. S., Park, K., Kang, E., Lee, S., Nam, H. Y., Kim, K., Park, J. H., Chi, D. Y., Park, R. W., Kim, I. S., Choi, K., and Kwon, I. C. (2008) Self-assembled glycol chitosan nanoparticles for the sustained and prolonged delivery of antiangiogenic small peptide drugs in cancer therapy. *Biomaterials 29*, 1920–1930.

(3) Zhang, N., Chittasupho, C., Duangrat, C., Siahaan, T. J., and Berkland, C. (2007) PLGA nanoparticle-peptide conjugate effectively targets intercellular cell-adhesion molecule-1. *Bioconjugate Chem. 19*, 145–152.

(4) Pasqualini, R., Koivunen, E., and Ruoslahti, E. (1997) α_v Integrins as receptors for tumor targeting by circulating ligands. *Nat. Biotechnol. 15*, 542–546.

(5) Fujikawa, L. S., Foster, C. S., Harrist, T. J., Lanigan, J. M., and Colvin, R. B. (1981) Fibronectin in healing rabbit corneal wounds. *Lab Invest. 45*, 120–129.

(6) Nishida, T., Nakamura, M., Murakami, J., Mishima, H., and Otori, T. (1992) Epidermal growth factor stimulates corneal epithelial cell attachment to fibronectin through a fibronectin receptor system. *Invest. Ophthalmol. Vis. Sci. 33*, 2464–2469.

(7) Rosenblatt, M. I., and Azar, D. T. (2004) Gene therapy of the corneal epithelium. *Int. Ophthalmol. Clin. 44*, 81–90.

(8) Carlson, E. R., Liu, C. Y., Yang, X., Gregory, M., Ksander, B., Drazba, J., and Perez, V. L. (2004) In vivo gene delivery and visualization of corneal stromal cells using an adenoviral vector and keratocyte-specific promoter. *Invest, Ophthalmol. Vis. Sci. 45*, 2194–2200.

(9) Tong, Y. C., Chang, S. F., Liu, C. Y., Kao, W., Huang, C. H., and Liaw, J. (2007) Eye drop delivery of nano-polymeric micelle formulated genes with cornea-specific promoters. *J. Gene Med. 9*, 956–966.

(10) Shi, M., Wosnick, J. H., Ho, K., Keating, A., and Shoichet, M. S. (2007) Immuno-polymeric nanoparticles by Diels-Alder chemistry. *Angew. Chem., Int. Ed. 46*, 6126–6131.

(11) Kolb, H. C., Finn, M. G., and Sharpless, K. B. (2001) Click chemistry: diverse chemical function from a few good reactions. *Angew. Chem. Int. Ed. 40*, 2004–2021.

(12) Alvarez, R., VelAzquez, S., San-Felix, A., Aquaro, S., De Clercq, E., Perno, C. F., Karlsson, A., Balzarini, J., and Camarasa, M. J. (1994) 1,2,3-Triazole-[2′,5′-bis-O(-tert-butyldimethylsilyl)-β-D-ribofuranosyl]-3′-spiro-5″-(4′-amino-l″,2″-oxathiole 2″, 2″-dioxide)(TSAO) analogues: synthesis and anti-HIV-1 activity. *J. Med. Chem. 37*, 4185–4194.

(13) Alagarsamy, V., Meena, S., Ramaseshu, K. V., Solomon, V. R., and Kumar, T. (2007) 4-Cyclohexyl-1-substituted-4*H*-[1,2,4]triazolo [4,3-*a*] quinazolin-5-ones: novel class of mH1-antihistaminic agents. *Chem. Biol. Drug Des. 70*, 158–163.

(14) Aufort, M., Herscovici, J., Bouhours, P., Moreau, N., and Girard, C. (2008) Synthesis and antibiotic activity of a small molecules libraryof 1,2,3-triazole derivatives. *Bioorg. Med. Chem. Lett. 18*, 1195–1198.

(15) Shi, M., and Shoichet, M. S. (2008) Furan-functionalized copolymers for targeted drug delivery: characterization, self-assembly and drug encapsulation. *J. Biomater. Sci.: Polym. Edit. 15*, 1143–1157.

(16) Vlerken, L., Vyas, T., and Amiji, M. (2007) Poly(ethylene glycol)-modified nanocarriers for tumor-targeted and intracellular delivery. *Pharm. Res. 24*, 1405–1414.

(17) Chen, X., McCarthy, S. P., and Gross, R. A. (1998) Synthesis, modification, and characterization of L-lactide/2,2-[2-pentene-1,5-diyl]trimethylene carbonate copolymers. *Macromolecules 31*, 662–668.

(18) Jeong, B., Kibbey, M. R., Birnbaum, J. C., Won, Y. Y., and Gutowska, A. (2000) Thermogelling biodegradable polymers with hydrophilic backbones: PEG-*g*-PLGA. *Macromolecules 33*, 8317–8322.

(19) Lee, L. A., Mitchell, M. L., Huang, S. J., Fokin, V. V. K., Sharpless, B., and Wong, C. H. (2003) A potent and highly selective inhibitor of human-1,3-fucosyltransferase via click chemistry. *J. Am. Chem. Soc. 125*, 9588–9589.

(20) Perez-Balderas, F., Ortega-Munoz, M., Morales-Sanfrutos, J., Hernandez-Mateo, F., Calvo-Flores, F. G., Calvo-Asin, J. A., Isac-Garcia, J., and Santoyo-Gonzalez, F. (2003) Multivalent neoglycoconjugates by regiospecific cycloaddition of alkynes and azides using organic-soluble copper catalysts. *Org. Lett. 5*, 1951–1954.

(21) Seo, T. S., Li, Z., Ruparel, H., and Ju, J. (2002) Click chemistry to construct fluorescent oligonucleotides for DNA sequence. *J. Org. Chem. 68*, 609–612.

(22) Parrish, B., Breitenkamp, R. B., and Emrick, T. (2005) PEG- and peptide-grafted aliphatic polyesters by click chemistry. *J. Am. Chem. Soc. 127*, 7404–7410.

(23) Montet, X., Funovics, M., Montet-Abou, K., Weissleder, R., and Josephson, L. (2006) Multivalent effects of RGD peptides obtained by nanoparticle display. *J. Med. Chem. 49*, 6087–6093.

(24) Herron, J. N., Gentry, C. A., Davies, S. S., Wei, A., and Lin, J. (1994) Antibodies as targeting moieties: affinity measurements, conjugation chemistry and applications in immunoliposomes. *J. Controlled Release 28*, 155–166.

(25) Mercadal, M., Domingo, J. C., Petriz, J., Garcia, J., and De Madariaga, M. A. (1999) A novel strategy affords high-yield coupling of antibody to extremities of liposomal surface-grafted PEG Chains. *Biochim. Biophys. Acta 1418*, 232–238.

(26) Koning, G. A., Morselt, H. W., Velinova, M. J., Donga, J., Gorter, A., Allen, T. M., Zalipsky, S., Kamps, J. A., and Scherphof, G. L. (1999) Selective transfer of a lipophilic prodrug of 5-fluorodeoxyuridine from immunoliposomes to colon cancer cells. *Biochim. Biophys. Acta. 1420*, 153–167.

(27) Xiong, X. B., Mahmud, A., Uludag, H., and Lavasanifar, A. (2007) Conjugation of arginine-glycine-aspartic acid peptides to poly(ethylene oxide)-b-poly(ε-caprolactone) micelles for enhanced intracellular drug delivery to metastatic tumor cells. *Biomacromolecules 8*, 874–884.

(28) Saxon, E., and Bertozzi, C. R. (2000) Cell surface engineering by a modified Staudinger reaction. *Science 430*, 873–877.

(29) Chaderjian, W. B., Chin, E. T., Harris, R. J., and Etcheverry, T. M. (2005) Effect of copper sulfate on performance of a serum-free CHO cell culture process and the level of free thiol in the recombinant antibody expressed. *Biotechnol. Prog. 21*, 550–553.

(30) Castel, S., Pagan, R., Mitjans, J., Piulats, J., Goodman, S., Jonczyk, A., Huber, H., Vilaró, S., and Reina, M. (2001) RGD peptides and monoclonal antibodies, antagonists of αv-Integrin, enter the cells by independent endocytic pathways. *Lab. Invest. 81*, 1615–1626.

(31) Aota, S., Nomizu, M., and Yamada, K. M. (1994) The short amino acid sequence Pro-His-Ser-Arg-Asnin human fibronectin enhances cell-adhesive function. *J. Biol. Chem. 269*, 24756–24761.

(32) Craig, J. A., Rexeisen, E. L., Mardilovich, A., Shroff, K., and Kokkoli, E. (2008) Effect of linker and spacer on the design of a fibronectin-mimitic peptide evluated via cell studies and AFM adhesion forces. *Langmuir 24*, 10282–10292.

BC8003167